INVESTIGATION OF THE CONDITION TO SYNTHESIZE HAp/CNTs COATINGS ON 316LSS

Nguyen Thi Thom[1, 2, *], Pham Thi Nam[1], Nguyen Thu Phuong[1], Dinh Thi Mai Thanh[2, 3]

[1]*Institute for Tropical Technology, VAST, 18 Hoang Quoc Viet, Cau Giay District, Ha Noi*

[2]*Graduate University of Science and Technology, VAST, 18 Hoang Quoc Viet, Cau Giay, District, Ha Noi*

[3]*University of Science and Technology of Hanoi, VAST, 18 Hoang Quoc Viet, Cau Gia, Ha Noi*

[*]Email: *ntthom@itt.vast.vn*

Received: 16 July 2018; Accepted for publication: 9 September 2018

ABSTRACT

Hydroxyapatite/carbon nanotubes (HAp/CNTs) nanocomposite was successfully synthesized as a coating on 316L stainless steel (316L SS) by electrodeposition technique. Effects of some factors such as: scanning potential range, scan rate, scan number, and synthesis temperature on the characteristic of the coatings were investigated. The characteristics of materials were determined by FT-IR, XRD, SEM, and mechanical test. Optimal conditions to synthesize HAp/CNTs/316L SS coatings are 0 ÷ -1.65 V/SCE of potential range, 5 mV/s, 5 scans at 45 ^{o}C. At the condition, obtained nanocomposite coatings are composed of HAp and CNTs with 6.9 µm of the coating thickness. The presence of 6.95 % of CNTs in the nanocomposite, the solubility of HAp/CNTs coatings is lower than pure HAp coating. In addition, the hardness of the HAp/CNTs coatings reaches 5.6 GPa, which was higher nearly 25 % in comparision with pure HAp.

*Keywords***:** hydoxyapatite (HAp), HAp/CNTs nanocomposite, electrodeposition, 316L SS.

1. INTRODUCTION

Nowadays, the demand for high quality biomedical materials is increasing due to the growth of injuries number. The most used biocompatible medical materials for surgery and orthopedics in hospitals are: 316L SS, CoNiCrMo, Ti and Ti6Al4V. Generally, the materials have excellent mechanical properties but in some cases they can be corroded in the biological environment after body implementation [1]. Therefore, new research to improve the quality of the biomedical materials based on metals and alloys are attracting scientists.

Hydroxyapatite (HAp) is a main component of bone tissue, has osteoconductive, biocompatible and excellent bioactive properties [2]. HAp can be used as bioactive coatings on the metals or alloys. However, high solubility in biological environments as well as poor

mechanical properties are disadvantage of HAp. The high solubility can reduce fixed capacity of implant materials with the host tissue [3]. So, the researchers incorporated in pure HAp reinforcing materials such as CNTs, TiO_2, ZrO_2 to overcome these disadvantage and to provide better corrosion resistance [4-6].

Carbon nanotubes (CNTs) is known as the material with excellent mechanical properties. So, they are used as a reinforcement for metals, alloys or polymers [7]. Some studies showed that the presence of CNTs significantly improved mechanical properties of pure HAp [1, 7, 8].

The scientists synthesized HAp/CNTs nanocomposite coatings by some methods such as: a Shear Mixing method [9], Plasma Sprayed [10], Electrophoretic Deposition [1, 11] and Electrodeposition [2, 8]. In which, electrodeposition is chosen to synthesize the thin coatings on the surface of metals and alloys. In 2013, D. Gopi et. al synthesized HAp/CNTs composite on Titanium and investigated the effect of CNTs amount on characteristic of obtained materials [2]. However, the authors have not yet investigated the effect of other factors as well as have not yet chosen the optimal condition to synthesize HAp/CNTs coatings.

In our previous report, the effect of CNTs amount was investigated and 0.5 g/L of CNTs is suitable [12]. In this work, HAp/CNTs nanocomposite coatings are synthesized on 316L SS by the electrodeposition. The effects of parameters such as scanning potential range, scanning rate, number of scans, and temperature on thickness, phase component, morphology and adhesion strength are investigated. The results show that HAp/CNTs nanocomposite improves the mechanical properties, the bioactivity and osteointegration of implants.

2. MATERIALS AND METHODS

2.1. Chemicals

The chemicals used in this work: $Ca(NO_3)_2.4H_2O$, $NH_4H_2PO_4$, $NaNO_3$ (99 % China). Multi-Walled carbon nanotubes (CNTs) (90 % pure, diameter 20 - 100 nm, length 1-10 µm) is a product of Insitute of Materials Science, Vietnam.

2.2. Substrate preparation

Table 1 showed element component of 316L SS substrate (100×10×2 mm). In our previous reports, 316L SS surface were treated and limited working area of $1cm^2$ [12].

Table 1. The element component of 316L SS alloy.

Element	Al	Mn	Si	Cr	Ni	Mo	P	Fe
Content (wt.%)	0.3	0.22	0.56	17.98	9.34	2.15	0.045	69.405

2.3. Carbon nanotubes preparation

Before the electrodeposition, CNTs were modified by chemical method [12].

2.4. Electrolyte preparation

In the previous report, 0.5 g/L is the optimal amount of CNTs amount of in the electrolyte solution. The amount of CNTs in HAp/CNTs/316L SS coatings was about 6.95 %. The presence of 6.95 % CNTs decreased about 35 % the disolution of the coatings [12].

In this work, the electrolyte solution containing 3×10^{-2} M of $Ca(NO_3)_2$,1.8×10^{-2} M of $NH_4H_2PO_4$, 0.15 M of $NaNO_3$ and 0.5 g/L of CNTs. pH solution is 4.4. $NaNO_3$ salt was used to improve conductivity of synthesis solution [13].

2.5. Electrodeposition process

The HAp/CNTs nanocomposite coatings were synthesized in 50 mL of electrolyte solution with a three-electrode cell: the working electrode (316L SS); a counter electrode (Platinum grid) and a reference electrode (Hg/Hg_2Cl_2/KCl-SCE). The electrodeposition was carried out on an AUTOLAB (Metrohm, Netherlands) with the change of scanning potential ranges: 0 to -1.6; 0 to -1.65; 0 to -1.7; 0 to -1.8; 0 to -1.9 and 0 to -2.0 V/SCE; scanning rates of 2, 3, 4, 5, 6 and 7 mV/s; number of scans of 3, 4, 5 and 6. The electrolyte temperature was kept at 30, 45 and 60 ^oC using a thermostated bath.

The masses of HAp/CNTs coatings were calculated by weighing of the substrate and obtained samples by a balance (XR 205SM-PR, Swiss).

The coating thickness is a result of an average of 5 measurements by Alpha-Step IQ devices (KLA-Tencor-USA).

The characteristics of the samples were investigated by FT-IR (IS10, NEXUS) using KBr pellet technique, in a range of 400 - 4000 cm^{-1} and 4 cm^{-1} resolution with 32 scans. The phase component was identified by XRD (SIEMENS D5005 Bruker-Germany, Cu-Kα, λ = 1.5406, 40 kV, 30 mA, 0.030 ^{o}/s). The analysis was mesured in a 2θ of 20°-70^o. The surface morphology of HAp/CNTs were characterized by SEM (Hitachi S-4800).

The coating dissolution was determined by the concentration of Ca^{2+} ions when they were immersed in 20 ml of NaCl (0.9 %) solution with the different time using Atomic Absorption Spectrometry (iCE 3500).

The adhesion strength between the coatings and the substrate was evaluated following an ASTM F1044 standard by tensile testing [14]. Surface roughness of the materials with and without HAp, HAp/CNTs coatings was determined by Atomic Force Microscopy (AFM). The hardness and elastic modulus of 316L SS coated with HAp, HAp/CNTs were determined by Mikrohärte - Prüfeinrichtung mhp 100 following TCVN - 258-1:2007 Vietnam standard and MTS 793 (g), USA.

3. RESULTS AND DISCUCIONS

3.1. Coating electrodeposition and characterization

3.1.1. Effect of scanning potential range

Fig. 1 shows the cathodic polarization curve of 316L SS in synthesis solution with 0.5 g/L of CNTs in a potential range from 0 to -2.0 V/SCE, 5 mV/s at 45 ^oC. At 0 to -0.7 V/SCE, the current density is approximately 0 according to the lack of electrochemical reactions. Then from -0.7 to -1.5 V/SCE, the current density slightly rises corresponding to the reduction of H^+, O_2 in

H_2O. In negative potential range than -1.5 V/SCE, the current density strongly rises due to the reduction of $H_2PO_4^-$ and H_2O to form PO_4^{3-} and OH^- [15].

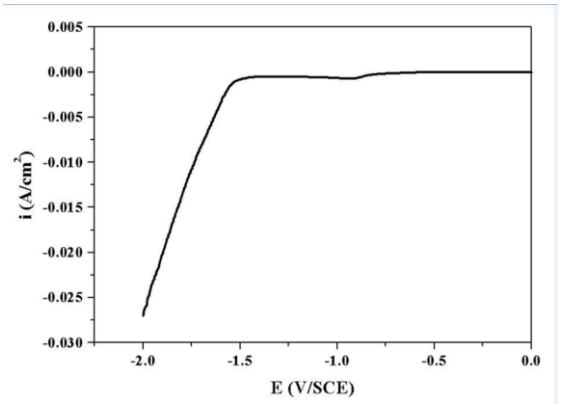

Figure 1. Cathodic polarization curve of 316L SS in the synthesis solution.

Table 2 shows the variation of some parameters of the obtained coatings. It is shown that the charge of HAp/CNTs synthesis process rises with the rise of potential range. More interesting, the mass rises and reaches a maximum value of 3.16 mg/cm^2 for the sample synthesized at 0 to -1.9 V/SCE corresponding to a thickness of 10.1 µm. Then the mass, as well as the thickness of the coatings, decreases when it is synthesized at 0 to -2.0 V/SCE.

Table 2. Some parameters of HAp/CNTs/316L SS materials synthesized at different potential ranges at 45 ^oC.

Potential range (V/SCE)	Charge Q (C)	Mass (mg/cm^2)	Thickness (µm) ISO 4288-1998	Adhesion strength (MPa)
0 ÷ -1.60	1.91	1.79	5.90	13.37
0 ÷ -1.65	2.05	2.10	6.90	13.20
0 ÷ -1.70	2.30	2.29	7.80	10.08
0 ÷ -1.80	4.09	2.78	9.00	9.40
0 ÷ -1.90	8.64	3.16	10.10	9.00
0 ÷ -2.00	9.39	2.26	7.30	6.70

The results of adhesion strength present that HAp/CNTs coatings synthesized at 0 ÷ -1.6 or 0 ÷ -1.65 V/SCE have the same value of the adhesion strength (13.37 and 13.2 MPa, respectively). This value decreases if the coatings are synthesized at more negative potential. It can be explained by the fact that at the negative potential range, the reduction of $H_2PO_4^-$ and HPO_4^{2-} is strong, H_2 gas is intensively generated. HAp/CNTs coatings become porous leading to the decrease of the adhesion strength value. Thus, 0 ÷ -1.65 V/SCE is suitable potential range to synthesize HAp/CNTs/316L SS.

FTIR spectra of HAp/CNTs coatings obtained at different potential range are similar and reveal charactersistic peaks of the IR active groups of HAp and CNTs (Figure 2). Streching vibrations of –OH of hydroxyapatite are characterized at 3440 cm^{-1} and 1640 cm^{-1}. The absorption peaks of PO_4^{3-} are observed at 1040; 560 and 600 cm^{-1}. In the spectrum of

HAp/CNTs composite have a shift of C-OH of CNTs from 1385 cm^{-1} to 1380 cm^{-1} due to the interaction between Ca^{2+} of HAp and COO^- group composing CNTs [2]. The results show the formation of the HAp/CNTs/316L SS.

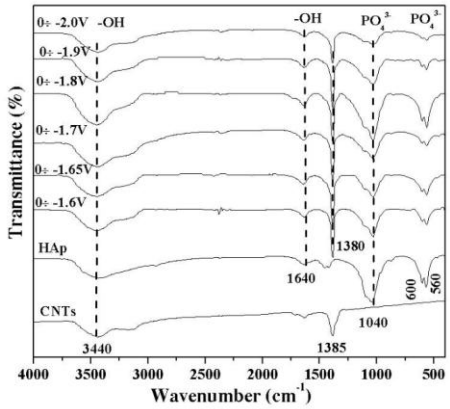

Figure 2. FTIR spectra of HAp/CNTs obtained with difeerent potential ranges at 45 ^oC.

The effect of potential range on the coating morphology is shown in Fig. 3. HAp/CNTs coatings have flake-like shape when they are synthesized in the potential range of 0 ÷ -1.6 V/SCE or -1.65 V/SCE. For a wider scanning potential range, large plate shapes are obtained because the generation of OH^- and PO_4^{3-} ions is more effective to the formation and crystallization of HAp/CNTs coating.

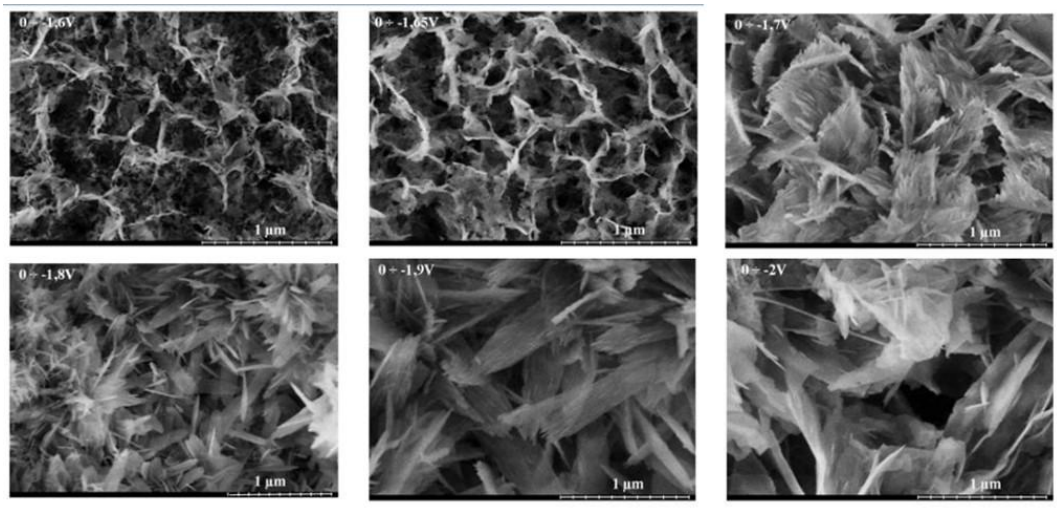

Figure 3. SEM images of HAp/CNTs synthesized with different potential ranges at 45 ^oC.

The phase component of HAp/CNTs obtained with the variation of the potential ranges is displayed in Figure 4. The X-ray diffraction pattern of HAp/CNTs synthesized in the range of 0 to -1.6 V/SCE displays the phases of HAp and CNTs. Additionally, the peaks corresponding to the dicalcium phosphate dihydrated (DCDP, $CaHPO_4.2H_2O$) are observed at $2\theta = 29.2^o$; 43^o; 51^o. The two phases obtained for this sample can be explained by the partial conversion of HPO_4^{2-} ions into PO_4^{3-}. Thus, the coating is composed of both HAp and DCPD.

At the wide potential ranges, HAp/CNTs coatings are composed characteristic peaks of HAp and CNTs. The diffraction peak with the highest intensity found at $2\theta = 31.77^{o}$ is corresponding to the (211) HAp crystal. The typical peak at 25.88^{o} of HAp is not observed because it is coinciding with the peak of CNTs at 26.3^{o} (002).

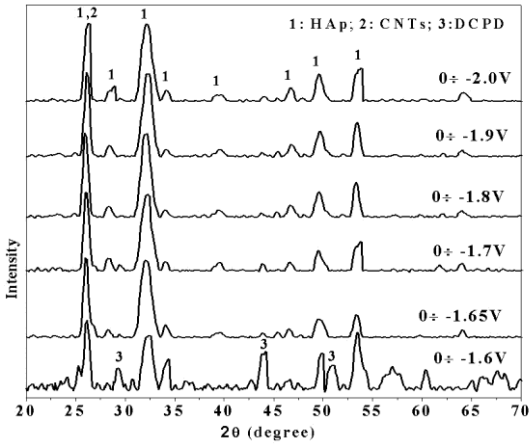

Figure 4. XRD patterns of HAp/CNTs synthesized with the variation of the potential ranges.

From the X-Ray diffraction patterns, HAp/CNTs crystallinity can be calculated (Table 4). We can see that the crystallinity of HAp/CNTs is high and rises with the openning of potential range because of a bigger amount of OH^{-} and PO_4^{3-} is created facilitating the HAp crystals.

Table 3. The variation of HAp/CNTs crystallinity following potential range.

Potential range (V/SCE)	Crystallinity (%)
0 ÷ -1.60	73.46
0 ÷ -1.65	85.40
0 ÷ -1.70	85.90
0 ÷ -1.80	86.90
0 ÷ -1.90	87.60
0 ÷ -2.00	88.10

From above results, the potential range of 0 to -1.65 V/SCE is chosen to synthesize HAp/CNTs/316L SS.

3.1.2. The effect of synthesis temperature

In this section, HAp/CNTs was synthesized with the variation of temperature from 30 ^{o}C to 60 ^{o}C. In Figure 5, the current density rises with the increasing of temperature. The charge of the synthesis process increases from 0.88 to 3.69 C when the temperature increases from 30 to 60 ^{o}C (Table 4).

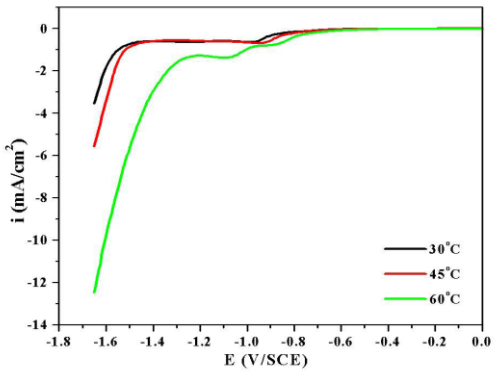

Figure 5. Cathodic polarization curves of 316L SS in the synthesis solution at different temperatures.

With the growth of temperature, the coating mass and coating thickness increase but the adhesion strength decreases (Table 4). The coatings synthesized at 45 ^{o}C are thicker than that synthesized at 30 ^{o}C (3.8 µm and 6.9 µm, respectively). However, the adhesion strength decreases slightly from 14.03 to 13.2 MPa. Especially, HAp/CNTs coatings synthesized at 60 ^{o}C have 12.2 µm thickness, but the adhesion strength decreases strongly and reaches 6.05 MPa. The results are explained by the temperature growth, the generation of larger amounts of OH^- and PO_4^{3-} ions and thus faster formation of HAp/CNTs on 316L SS. On the contrary, the rise of the temperature can promote the reduction of $H_2PO_4^-$ to generate H_2 gas on the working electrode surface leading to the decrease of adhesion strength value. So, the temperature at 45 ^{o}C was chosen to synthesize HAp/CNTs coatings for further studies.

Table 4. Some parameters of HAp/CNTs/316L SS material in function of the temperature.

Temperature (^{o}C)	Charge Q (C)	Mass (mg/cm^2)	Thickness (µm)	Adhesion strength (MPa)
30	0.88	1.16	3.80	14.03
45	2.05	2.10	6.90	13.20
60	3.69	3.73	12.20	6.05

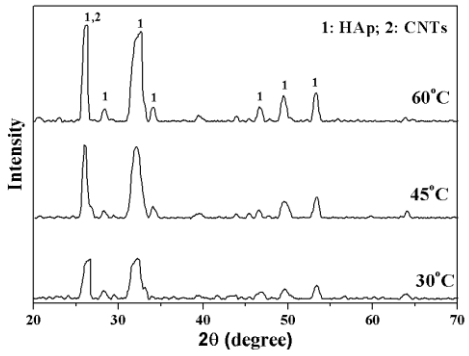

Figure 6. XRD patterns of HAp/CNTs in function of the temperature.

The X-Ray diffraction patterns show that the temperature does not affect the phase component of HAp/CNTs coatings (Figure 6). The obtained coatings are composed of HAp and CNTs. The typical peak observed at $2\theta = 31.77^{o}$ and corresponding to (211) plane confirms the presence of HAp and the peak at $2\theta = 26.3^{o}$ (002) confirms the one of CNTs.

The morphology of HAp/CNTs/316L SS deposited at the different temperature has cactus-like (Figure 7). HAp/CNTs coating obtained at 30 ^{o}C has flake-like and is arranged to form coral-like product. At 45 ^{o}C and 60 ^{o}C, HAp/CNTs coatings synthesized are uniform and tightly cover the 316L SS.

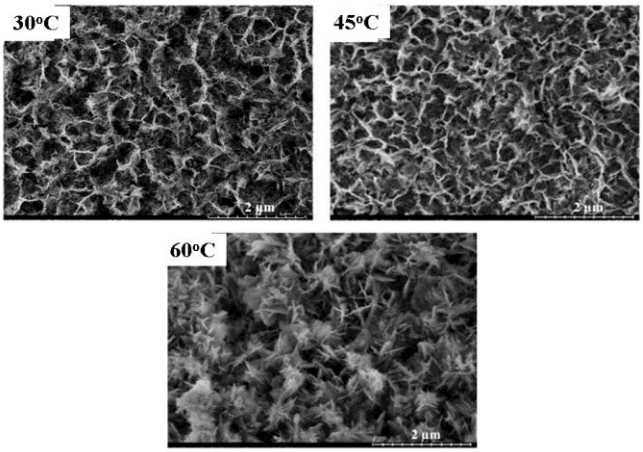

Figure 7. SEM images of HAp/CNTs/316L SS synthesized at different temperatures.

3.1.3. Effect of scan numbers

In this section, HAp/CNTs coatings were synthesized with 3, 4, 5 and 6 scans corresponding to the different charge 1.16; 1.61; 2.05 and 2.64 C. Other conditions are fixed: 0 ÷ -1.65 V/SCE, 5 mV/s at 45 ^{o}C.

The variations of some parameters of HAp/CNTs coatings are displayed in Table 5.

Table 5. Variation of some parameters of HAp/CNTs/316LSS as funtion of scan numbers.

Scans	Charge Q (C)	Mass (mg/cm^2)	Thickness (µm) ISO 4288-1998	Adhesion strength (MPa)
0		0	0	15.00
3	1.16	1.03	3.4	14.50
4	1.61	1.72	5.6	13.34
5	2.05	2.10	6.9	13.20
6	2.64	2.69	8.8	8.60

The data show that a larger number of scans causes leading to the increase of mass, thickness, and the decrease of adhesion strength. With 3 scans, the adhesion value is 14.5 MPa. It is the similar value of glue with 316L SS (15 MPa), because HAp/CNTs coatings are formed

less and are not able to cover completely the surface (mass about 1.03 mg/cm^2). When the charge increases and reaches 1.61 or 2.05 C (4 or 5 scans), coatings are uniform and thick, and the adhesion strength reaches about 13 MPa. The adhesion strength remarkably decreases to 8.6 MPa when the coatings were synthesized with 6 scans. At the charge of 2.64 C the HAp/CNTs coatings are non-uniform and porous. Thus, the optimal scanning time for further studies is 5 scans.

X-Ray diffraction patterns show that at different scan numbers, the obtained coatings are crystalline with single phases of HAp and CNTs, as can be seen in Figure 8. The percentage of crystallinity of HAp in coatings is presented in Table 6. It was observed that a higher scan number leads to the increase of the process charge and improves crystallinity. This value raises from 69.79 % to 86.1 % when the scan number increases from 3 to 6.

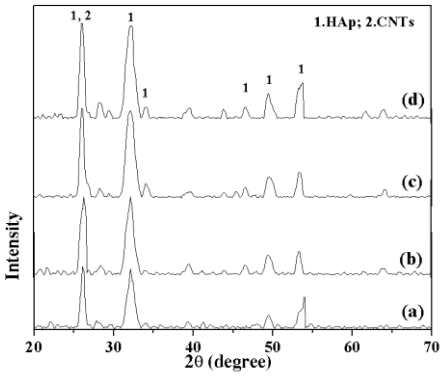

Figure 8. XRD patterns of HAp/CNTs synthesized with different scan numbers: (a) 3; (b) 4; (c) 5 and (d) 6 scans.

Table 6. The crystalline of HAp synthesized at different scan numbers.

Scans	3	4	5	6
The crystalline (%)	69.79	82.20	85.40	86.10

3.1.4. Effect of scanning rate

Table 7. The variation of parameters of HAp/CNTs/316L SS synthesized at 0 to -1.65 V/SCE, 5 scans at 45 ^{o}C with the different scanning rates.

Scanning rate (mV/s)	3	4	5	6	7
Charge Q (C)	3.97	2.71	2.05	1.70	1.10
Mass (mg/cm^2)	2.71	2.21	2.10	1.54	1.28
Adhesion strength (MPa)	9.6	12.85	13.2	13.42	14.02

Scanning rate is an important factor in electrochemical deposition, affecting the formation of the coatings. Thus, in this study the scanning rates were changed from 3 to 7 mV/s. Table 7 shows the characterization parameters of obtained coatings. With the rise of the scanning rate, the charge and mass decrease, however the adhesion strength increases. It can be explained by the low

charge of electrodeposition process. The smaller amounts of OH^- and PO_4^{3-} are generated leading to the reduction of coatings mass. At high charge (4.73 and 3.97 C), the big amounts of H_2 gas are generated on the 316L SS surface causing the porosity of HAp/CNTs coatings, and the decrease of the adhesion strength. Therefore, 5 mV/s of the scanning rate is suitable to synthesize HAp/CNTs/316L SS material.

The phase component of HAp/CNTs synthesized with the different scanning rates from 3 to 7 mV/s is displayed in Figure 9. It is clearly that the scanning rate does not affect the phase component of the coatings. The diffraction patterns for HAp/CNTs coatings reveal the phase of both HAp and CNTs.

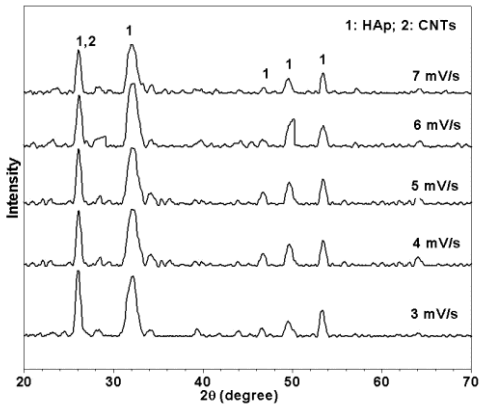

Figure 9. XRD patterns of HAp/CNTs synthesized with different scanning rates.

Based on the obtained results, we propose the optimal conditions for the synthesis of HAp/CNTs/316L SS coatings such as: the potential range of 0 ÷ -1.65 V/SCE, 5 mV/s, 5 scans, a temperature about 45 ^oC and 0.5 g/L of CNTs in the synthesis solution. In the next studies, the mechanical properties of the coatings with and without CNTs are determined.

3.2 Mechanical properties of the coatings

3.2.1 Material roughness

The values of roughness (Ra) estimated for 316L SS without and with HAp, HAp/CNTs coatings are 21 ± 2 nm, 241± 20 nm and 172 ± 20 nm, respectively. Figure 10 reveals the photography of coatings. The results show a significant change in the surface roughness of different coatings. The roughness of HAp coating is higher about ten times in comparison with 316L SS. With the presence of CNTs in the coating causes the decrease of roughness reaching 172 ± 20 nm. It means that CNTs improves significantly the roughness of HAp/CNTs coatings because HAp/CNTs coatings are uniform and tight.

3.2.2 Material elastic modulus

After estimation of the roughness, the coatings elastic modulus was calculated. Elastic modulus is the ratio of tensile stress and deformation of the material. The dependence of the tensile stress according to the deformation of the following materials: 316L SS, 316L SS with HAp or HAp/CNTs on the surface with pulling speed of 0.03 mm/s is linear. The equations for

materials listed above are presented as follow: y = 82246x + 2.1493 (R^2 = 0.9994); y = 86247x + 2.25393 (R^2 = 0.9991) and y = 92587x + 2.1495 (R^2 = 0.9995), see Figure 11.

The slopes are 82246, 86247 and 92587 which correspond to the elastic modulus of the materials. Indeed, 316L SS has the elastic modulus of about 82246 MPa ~ 82 GPa. This value increases to 86 GPa when 316L SS is covered by HAp coatings. The elastic modulus reaches about 92 GPa with the presence of 6.95 % CNTs in HAp/CNTs/316L SS. This result proves that CNTs can improve the elastic modulus of the HAp/CNTs coatings.

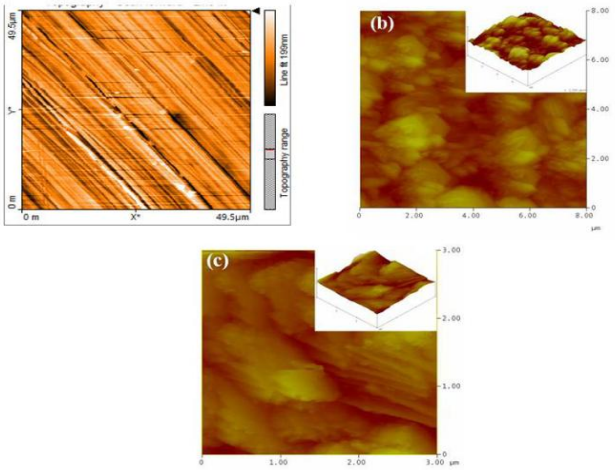

Figure 10. AFM images of (a) 316L SS, (b) HAp/316L SS and (c) HAp/CNTs/316LSS.

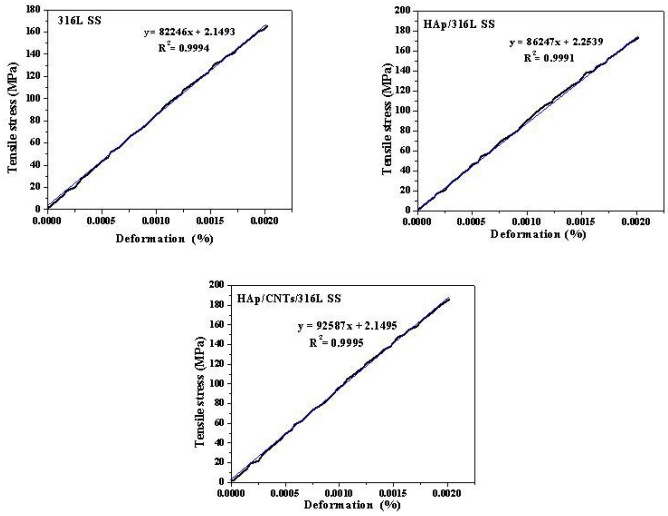

Figure 11. Relationship between the tensile stress and the deformation of the materials.

3.2.3. Materials hardness

The hardness of HAp/316L SS and HAp/CNTs/316L SS, with a thickness of about 8.5 µm and 6.9 µm respectively, were determined by Vickers method. The results show that the coating hardness without CNTs (HAp/316L SS) is 460 kgf/mm^2 (4.5 GPa). It is lower than the one with

CNTs (HAp/CNTs/316L SS), that is equal to 573 kgf /mm^2, 5.6 GPa. Thus, hardness of the coating with CNTs 0.5 g/L increases about 25 % in comparision with the coating without CNTs.

4. CONCLUSIONS

In this work, the optimal conditions to synthesize HAp/CNTs/316L SS were reported. The XRD results confirmed the crystallinity of the obtained HAp/CNTs coatings with the signals corresponding to the single phase of HAp at $2\theta = 31.77^o$ and CNTs at $2\theta = 26.3^o$, with 6.95 % of CNTs in the coatings. The crystallinity and the composition of the coatings depend on the electrodeposition conditions. CNTs increased the coating mechanical properties such as the adhesion strength, hardness and elastic modulus, while the surface roughness and dissolution of coatings decrease.

REFERENCES

1. Kaya C. - Electrophoretic deposition of carbon nanotube-reinforced hydroxyapatite bioactive layers on Ti–6Al–4V alloys for biomedical applications, Ceramics International **34** (2008) 1843–1847.
2. Gopi, D., Shinyjoy E., Sekar M., Surendiran M., Kavitha L., Sampath Kumar T.S. - Development of carbon nanotubes reinforced hydroxyapatite composite coatings on titanium by electrodeposition method, Corrosion Science **73** (2013) 321–330.
3. Baronov S. M., Tumanov S. V., Fadeeva I. V., Bibikov V. Y. - Environment effect on the sttength of hyroxy-and fluorohydroxyapatite ceramics, Inorg Mater **39** (2003) 877-880.
4. Sridhar T.M., Mudali U.K., Subbaiyan M. - Sintering atmosphere and temperature effects on hydroxyapatite coated type 316L stainless steel, Corros. Sci. **45** (2003) 2337–2359.
5. Chen X.H., Chen C.S., Xiao H.N., Cheng F.Q., Zhang G., Yi G.J.- Corrosion behavior of carbon nanotubes-Ni composite coating Surf. Coat. Technol. **191** (2005) 351–356.
6. Praveen BM, Venkatesha TV, Naik YA, Prashantha K. - Corrosion studies of carbon nanotubes–Zn composite coating, Surf. Coat. Technol. **201** (2007) 5836–5842.
7. Ashley A. W., Serena M. B., and Lan A. K. - Hydroxyapatite–carbon nanotube composites for biomedical applications: A review, Int. J. Appl. Ceram. Technol. **4** (2007) 1–13.
8. Xibo P., Yongxiang Z., Rui H., Zhongjie L., Lingyang T., Jian W., Qianbing W., Xiaoyu L., and Hong B. - Single-walled carbon nanotubes/hydroxyapatite coatings on titanium obtained by electrochemical deposition, Applied Surface Science **295** (2014) 71-80.
9. Susmita M., Biswanath K., Swarnendu S., and Abhijit C. - Improved properties of hydroxyapatite–carbon nanotube biocomposite: Mechanical, in vitro bioactivity and biological studies, Ceramics International **40** (2014) 5635–5643.
10. Kantesh B., Rebecca A., Tapas L., Melanie A., Jorge T., Eric C., and Arvind A. - Plasmasprayed carbon nanotube reinforced hydroxyapatite coatings and their interaction with human osteoblasts in vitro, Biomaterials **28** (2007) 618–624.
11. Długon E., Niemiec W., Frazek-Szczypta A., Jelen´P., Sitarz M., and Błazewicz M. - Spectroscopic studies of electrophoretically deposited hybrid HAp/CNT coatings on

titanium, Spectrochimica Acta Part A: Molecular and Biomolecular Spectroscopy **133** (2014) 872–875.

12. Thom N. T., Nam P. T., Thu Phuong N., Hong C. T., Trang N. V., Xuyen N. T., Mai Thanh D. T. – Eectrodeposition of hydroxyapatite/functionalized carbon nanotubes (HAp/fCNTs) coatings on the surface of 316L stainless steel, Vietnam Journal of Science and Technology **55** (6) (2017) 706-715.
13. Ren F., Xin R., Ge X., Leng Y. - Characterization and structural analysis of zinc-substituted hydroxyapatites, Acta Biomaterialia **53** (2009) 141-3149.
14. ASTM International, Standard test method for shear testing of calcium phosphate coatings and metallic coatings, ASTM F1044, ASTM International, West Conshohocken, Pa, USA, 2005, https://www.astm.org/DATABASE.CART/HISTORICAL/F1044-05.htm.
15. Thanh D. T. M., Nam P. T., Phuong N. T., Que L. X., Anh N. V., Hoang T., Lam T. D. - Controlling the electrodeposition, morphology and structure of hydroxyapatite coating on 316L stainless steel, Materials Science and Engineering C **33** (2013) 2037–2045.